ELSEVIER

International Journal of Adhesion & Adhesives 21 (2001) 389–396

International Journal of Adhesion & Adhesives

www.elsevier.com/locate/ijadhadh

Fracture toughness of spherical silica-filled epoxy adhesives

Makoto Imanaka[a,*], Yoshihiro Takeuchi[b], Yoshinobu Nakamura[c], Atushi Nishimura[c], Takeo Iida[c]

[a] *Osaka University of Education, Asahigaoka Kashiwara City, Osaka 582-8582, Japan*
[b] *Yonago Technical High School, Hakuro-cho, Yonago City, Tottiri 083-0052, Japan*
[c] *Department of Applied Chemistry, Osaka Institute of Technology, Ohmiya, Asahi-ku, Osaka 535-8585, Japan*

Accepted 7 March 2001

Abstract

Crack propagation in epoxy adhesives filled with spherical silica was investigated using double cantilever beam (DCB) specimens. In particular, to clarify the effect of particle size and particle/matrix adhesion upon the fracture toughness, silica particles were prepared with mean particle sizes in the range of 6–30 μm, where the particles were treated with γ-aminopropyl methyldiethoxysilane and hexamethyl disilazane. The former and latter treatments demonstrated well- and poorly-bonded interfaces between the particle and matrix, respectively. The experimental results showed that the fracture toughness of DCB specimens increases with particle size and with interfacial strength of silica/matrix depending on the particle content. The behavior has been interpreted in terms of crack pinning and crack blunting.

Keywords: Adhesive joint; Fracture toughness; Double cantilever beam specimen; Spherical silica; Epoxy adhesive

1. Introduction

Epoxy resins are widely employed as the basis for adhesive components because they have many useful engineering properties such as a relatively high modulus and strength. However, pure epoxy resins are relatively brittle polymers with poor resistance to crack propagation. To improve the crack resistance of epoxy resins, inorganic fillers have been widely used. Hence, there have been many studies of the mechanical properties and fracture mechanism of these filled epoxy resins [1,2]. In the early stage, most studies of filled resins were concerned with static properties, i.e., Young's modulus, yield stress and so on [3,4]. Recently, the main focus has shifted to crack propagation properties. In particular, the fracture toughness of silica and glass bead-filled epoxy resin has attracted special interest [5–11]. Concerning fracture toughness of filled resins, there are two important toughening mechanisms, one is crack pinning and another is crack tip blunting. According to the crack pinning mechanism the propagating crack is impeded by rigid particles [12,13]. While, blunting at the crack tip can take place through localized shear yielding and the formation of a damage zone due to crack diversion, particle fracture, and debonding of the particle/matrix interface [10,11]. In the above studies, the effect of particle size, content and particle/matrix adhesion on fracture toughness have been discussed based on crack pinning and crack tip blunting mechanisms.

As described above, fracture toughness of the filled resins has been investigated in detail. There have been few studies of the fracture toughness of adhesive joints using these filled adhesives, though there are many different points of fracture characteristics between adhesive joints and bulk resins. It is necessary to clarify the effect of filling conditions on fracture toughness of adhesive joints. Concerning the filling conditions, the bonding strength of the particle/matrix interface is an important parameter determining which mechanism is dominant in the filling system, pinning or crack tip blunting. Because strengthening the particle/matrix adhesion increases the efficiency of pinning but suppresses crack tip blunting. In this study, to clarify the bonding condition of the interface, spherical silica particles were treated with γ-aminopropyl methyldiethoxysilane and hexamethyl disilazane, where the former strengthens and the latter weakens the bond strength of the interface. Using these treated silica

*Corresponding author.

0143-7496/01/$ - see front matter
PII: S0143-7496(01)00016-1

particles as filling materials of the adhesives, the effect of particle size, content and particle/matrix adhesion on fracture toughness was investigated using adhesively bonded double cantilever beam (DCB) specimens. The experimental results were interpreted in terms of crack pinning and crack blunting mechanisms.

2. Experimental procedure

2.1. Adhesives and adhesively bonded joint specimens

The mean sizes of silica particles used in this study were 6, 11, 17 and 30 μm (FB-6S, FB-35, FB48, FB-74, Denkikagaku-kogyo, Co. Ltd.). These silica particles were spherical, hence sizes of the particle indicates the diameter of the particle. To increase and decrease the adhesion between the particles and matrix, silica particles were treated with γ-aminopropyl methyl-diethoxysilane and hexamethl disilazane, respectively. Hereafter, these treatments are abbreviated to APDES and HMDS, respectively. The epoxy resin used was bisphenol-A type epoxy resin (Epikote 828, Shell Chemical Co. equivalent weight per epoxy group 190 ± 5, average molecular weight 380). Piperidine was used as a curing agent.

Fig. 1 shows the shape and sizes of the adhesively bonded double cantilever beam (DCB) specimen whose adherend is structural carbon steel (JIS S55C). As shown in Fig. 1(a) filler gauge 0.01 mm thick inserted between Teflon sheets of 0.1 mm thickness was used for the pre-crack, where the filler gauge was treated by a release agent. Adhesive layer thickness was adjusted to 0.21 mm by the pre-crack and a Teflon spacer at the end of the bond line. Surface preparation for adhesion was as follows: The adherend was polished with #180 mesh emery paper, and the polished surface was rinsed in 2% methanol solution of a siliane coupling agent (KBM403, Sinetukagaku-kogyo, Co. Ltd.), then dried at room temperature and heated at 373 K for 5 min. The DCB specimens were finally cured for 20 h at 375 K. After curing, the edges at the bond line were polished.

2.2. Tensile test

Load–unloading testing of the DCB specimens was conducted in a chamber controlled to 294 ± 1 K, with a crosshead speed of 3 mm/min and displacement of the loading point measured by a clip gauge. The energy release rate was calculated from the following equation [14]:

$$G = \frac{P^2 \mathrm{d}C}{2B\mathrm{d}a}, \tag{1}$$

where P is the load at peak point, C is the compliance, B is the width of the specimen, and a is the crack length. Based

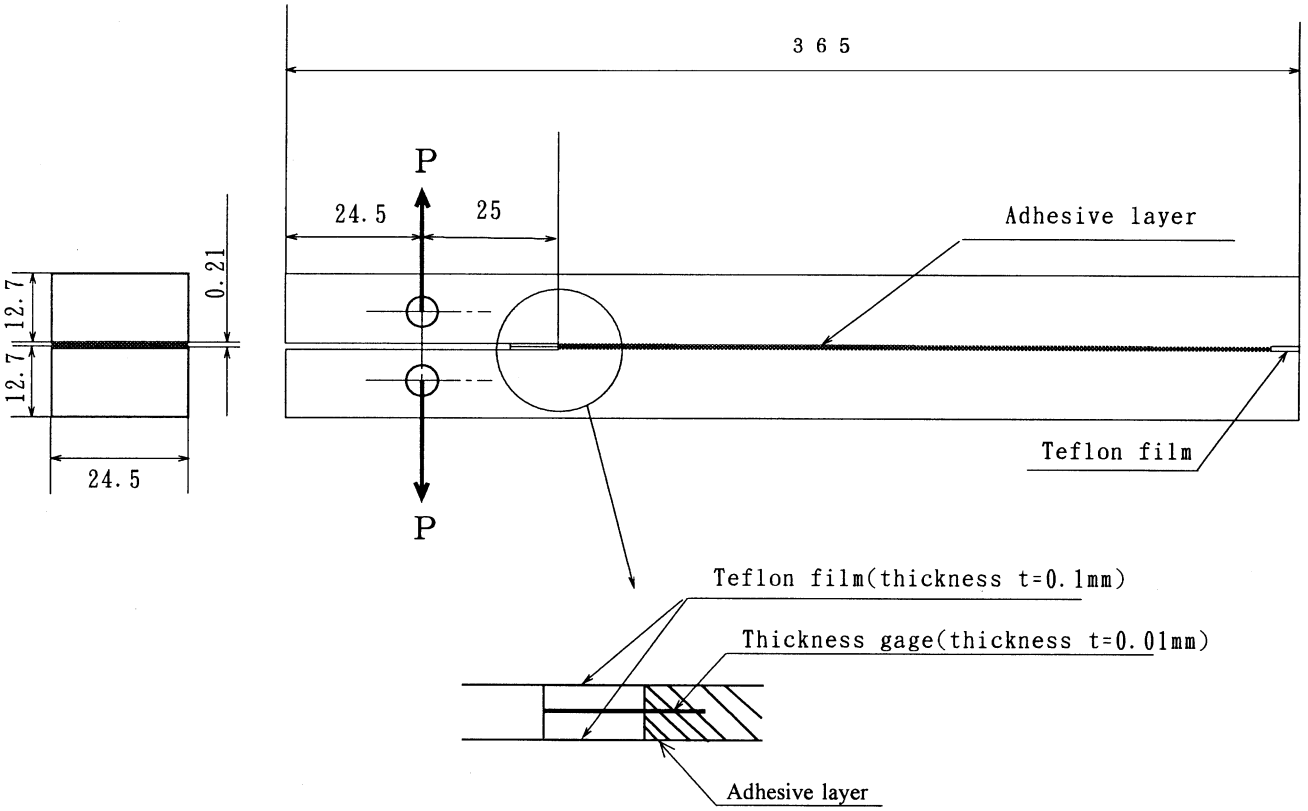

Fig. 1. Shape and sizes of the adhesively bonded DCB specimen.

on the simple beam theory, the value of the compliance, C, is given by [14],

$$C = \frac{2a^3}{E_s I}, \tag{2}$$

where E_s is the flexural modulus of the adherend and I is the second moment of the area. However, compliance of the actual DCB specimen is affected by the rotation and deflection at the crack tip, and so on. Backman et al. [15] evaluated the actual compliance of the DCB specimen using some correction factors as follows:

$$\left(\frac{C}{N}\right)^{1/3} = \left(\frac{2}{3IE_s}\right)(a + \chi h), \tag{3}$$

where N and χ are the correction factors, h is the thickness of the adherend. Eq. (3) indicates that there is a linear relationship between a and $C^{1/3}$. Backman et al. recommended the calculation of dC/da based on Eq. (3). In this experiment, a linear relationship between a and $C^{1/3}$ was also observed as shown in Fig. 2. Hence, the calculation of dC/da was conducted based on Eq. (3).

Experimental results showed that the fracture pattern varied from cohesive fracture to interfacial fracture as the crack length increased. Fracture mechanisms of cohesive fracture differ from those of interfacial fracture. Furthermore, calculated fracture toughness corresponding to interfacial fracture was less than half the fracture toughness of cohesive fracture. Hence, when calculating the energy release rate, critical loads for interfacial fracture were excluded, and only peak loads for cohesive fracture were adopted. Furthermore the first peak of load–deflection curves was also excluded, for it corresponded to the critical load for crack propagation from the artificial pre-crack. Beside, data plots of fracture toughness in this paper indicated the average of five measurements.

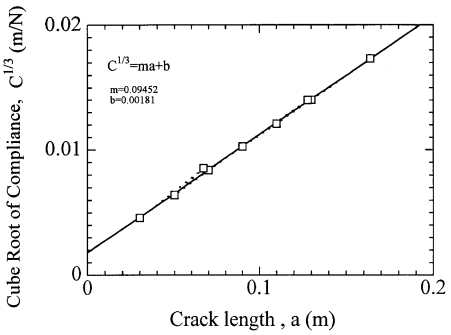

Fig. 2. Experimental compliance–crack length calibration results for a DCB specimen (unfilled epoxy adhesive: adhesive layer thickness $t = 0.2$ mm).

To compare the fracture toughness of the DCB specimen with that of the bulk specimen, the fracture toughness of the bulk specimen was also measured by a single notched beam loaded in a three-point bending test according to ASTM D5048-91. Young's modulus and Poisson's ratio of the bulk specimen were also measured by a three-point bend test according to ASTM D790 and by a tensile test of a plate specimen (width: 25 mm, thickness 2 mm) attached to two directional strain gages in the middle of the plate, respectively. The detailed conditions of the three-point bending test for the bulk specimen are shown in the previous papers [11].

To compare the fracture toughness of the DCB specimen with that of the bulk specimen, the energy release rate of the DCB specimen was translated into the stress intensity factor using Eq. (3) [14]:

$$K = \sqrt{\frac{GE}{(1 - \nu^2)}}. \tag{4}$$

Here, G is the energy release rate, E is Young's modulus, and ν is Poisson's ratio. Young's modulus and Poisson's ratio of the bulk specimen are shown in Table 1.

3. Results and discussion

3.1. Stability of crack propagation

Fig. 3 shows examples of load–displacement curves for DCB specimens bonded by unfilled and HMDS-treated silica particle-filled epoxy adhesives. As shown in this figure, both untreated and HMDS-treated systems

Table 1
Mechanical properties of bulk adhesives (silica particles treated with HMDS)

Silica content (wt%)	Mean particle size (μm)	Young's modulus (MPa)	Poisson's ratio
0		3190	0.38
6.25	6	3201	0.36
6.25	17	3230	0.36
6.25	30	3150	0.36
12.5	6	3620	0.36
12.5	17	3520	0.36
25	6	4090	0.35
25	17	4050	0.36
25	30	4020	0.36

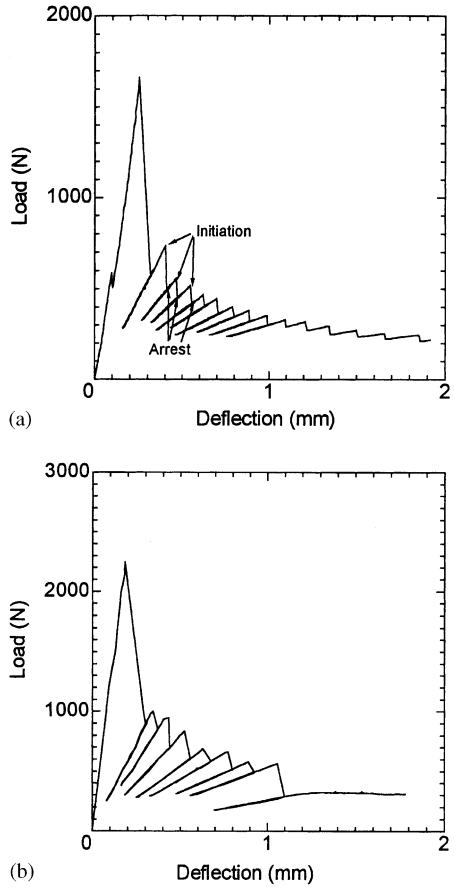

Fig. 3. Typical load–deflection curves trace for the DCB specimen; (a) unfilled epoxy adhesive, (b) epoxy adhesive filled with HMDS-treated spherical silica.

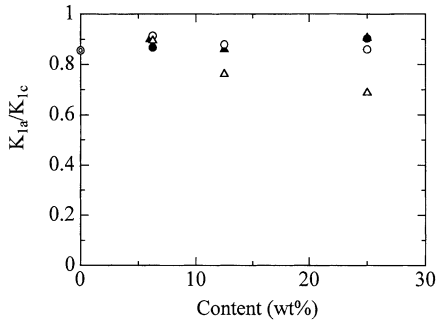

Fig. 4. K_{Ia}/K_{Ic} vs. silica content for DCB specimens.

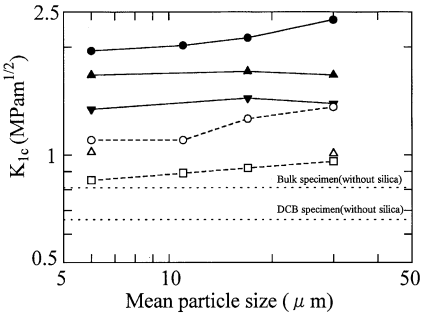

Fig. 5. Effect of mean particle size on fracture toughness where silica particles were treated with HMDS. Filled points are for bulk specimens and open points for DCB specimens.

show typical unstable stick-slip type propagation behavior, which were observed for all kinds of DCB specimens in this study. Stress intensity factors for initiation and arrest, $K_{Ia}$and K_{Ic} were derived from the initiation and arrest loads as shown in Fig. 3(a). To evaluate the stability of crack propagation, the ratios of arrest load to critical load for crack propagation, K_{Ia}/K_{Ic}, are shown in Fig. 4. In the case of stable propagation, $K_{Ia}/K_{Ic} = 1$ and K_{Ia}/K_{Ic} decreases with increasing instability of crack propagation. This figure shows that K_{Ia}/K_{Ic} is independent of silica content and surface treatment of silica particles except for adhesives containing HMDS-treated silica particles with a mean size of 6 μm. In contrast, K_{Ia}/K_{Ic} of adhesives containing HMDS-treated 6 μm silica particles decreases with increasing silica content. For several particle-filled resins, it was reported that unstable crack propagation occurred at certain contents of particles even though propagation was always continuous in an unfilled system, and that the stability of crack propagation varied with filler content and surface treatment of the particles [6,7]. In this system as shown in Fig. 4, crack propagation stability was not clearly depend on filler content and surface treatment of particles. One reason may be the difference in the crack propagation stability of the unfilled system between bulk resins in the above reports and DCB specimens in this study.

3.2. Effect of particle size and weight fraction

Fig. 5 shows the effect of particle size on critical stress intensity factor K_{Ic} for DCB and bulk specimens indicating the content of the silica particles as a parameter, in addition to the bulk data with 50 wt% measured in the previous paper [16]. This figure shows that the fracture toughness of the bulk specimens is about 1.2–1.6 times higher than that of the DCB specimen for both filled and unfilled systems. Generally, positive and negative hydrostatic stresses make most of the polymeric materials ductile and brittle, respectively [14]. For adhesively bonded DCB specimens, a high degree of negative hydrostatic pressure is applied in the vicinity of the crack tip due to restraint on the adherend, which may reduce the fracture toughness of the DCB specimens. This figure also shows that the fracture toughness of the bulk specimen with content of 50 wt% and the DCB specimen with content of 25 wt% increase remarkably with particle size. However, the effect of particle size on fracture toughness weakens with decreasing content of silica particles for both the DCB and bulk specimens. Furthermore, the dependency of fracture toughness on the particle size of the DCB

specimen is more remarkabl than that of the bulk specimen with the same silica content.

There is no certain trend between silica size and fracture toughness of bulk resin. However, in many previous papers it has been confirmed that the toughness of bulk resins increases with particle size for high particle contents [8,9,11]. Especially in a report of fracture toughness test of spherical silica-filled epoxy resin, it was confirmed that an increase of the silica size prompted crack diversion and debonding of the particle/matrix interface from the observation of the fracture surfaces of silica-filled resin samples. This means that increased particle size strengthens the effect of crack tip blunting [11]. Furthermore, the increase of silica content may strengthen such a blunting mechanism. Such a trend is also observed in Fig. 5, that is, the fracture toughness increases remarkably with particle size in the range of high silica content. Hence, in this experiment, the crack blunting may have been the main cause for the increase of fracture toughness with particle size.

Another main reinforcement mechanism for particle-filled resin is a pinning theory developed by Evans and Green [12,13], in which crack propagation energy from the secondary semi-elliptical cracks between particles was calculated. This theory leads to the following results: the ratio of stress intensity factor K_{Ic} (particle filled)/K_{Ic} (unfilled) depends on the ratio of particle diameter to the inter-particle separation d_p/D_s which is only a function of volume fraction of the particles V_p.

To investigate the effectiveness of the pinning theory, the ratios K_{Ic} (particle filled)/K_{Ic} (unfilled) are plotted against the ratios d_p/D_s in Fig. 6, where the values of d_p/D_s were calculated from Eq. (4) and V_p is the volume fraction of the silica particles [17]:

$$\frac{d_p}{D_s} = \frac{3V_p}{2(1\text{-}V_p)}. \quad (5)$$

The dotted lines represent the theoretical predictions for interacting and non-interacting elliptical cracks calculated by Green et al. [13]. Fig. 6 shows that at lower values of d_p/D_p the experimental data are close to the upper theoretical line, but close to the lower line at higher values of d_p/D_p for both DCB and bulk specimens. Besides, the average values of the DCB specimens agree well with those of the bulk specimen.

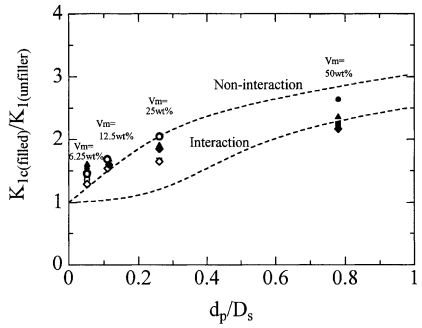

Fig. 6. Variation of K_{Ic} (silica filled)/K_{Ic} (unfilled) with d_p/D_s. The dashed lines represent theoretical predictions by Green et al. [13]. Filled points are for bulk specimens and open points for DCB specimens.

A similar trend of d_p/D_p, that is, the experimental data distributed between upper and lower theoretical lines, was obtained by Spanoudakis [5] and Kinloch et al. [7] for particle-filled epoxy resins. A close examination of this figure indicates that K_{Ic} (particle filled)/K_{Ic} (unfilled) decreases with decreasing particle size, and the effect of particle size on the stress intensity factor weakens with decreasing volume fraction of the silica particles. These trends imply that effectiveness of crack blunting diminishes and the pinning mechanism dominates with decreasing volume fraction of silica particles.

The macroscopic fracture surfaces of DCB specimens bonded by adhesives unfilled and 6- and 30-μm HMDS-treated particles filled are shown in Fig. 7. As shown in Fig. 7(a), the fracture surface of the unfilled adhesive presents fine 'thumbnail' lines corresponding to crack arrest lines running perpendicular to the direction of crack growth. In Fig. 7(b) which is a fracture surface filled with 6 μm particles, many irregular lines appear. Furthermore, as shown in Fig. 7(c), the density of the irregular lines in 30 μm particle-filled adhesive is greater than that in 6 μm particle-filled adhesive. This indicates that the density of the irregular lines increases with silica particle size, i.e. fracture toughness increases with the density of irregular lines which may relate to detours and branches of the crack. A similar relationship between the density of irregular lines in the fracture surface and fracture toughness has been observed for adhesive joints bonded by rubber-modified adhesives [18].

3.3. Effect of surface treatment of the silica particles

To investigate the effect of particle/matrix adhesion on the fracture toughness, the stress intensity factor of the DCB and bulk specimens filled with APDES treated (good bond) and HMDS-treated (poor bond) particles are shown in Fig. 8. As shown in this figure, the fracture toughness of bulk specimens does not depend on surface treatment of the silica particles. However, the critical stress intensity factor for the DCB specimens bonded by APDES-treated-particle filled adhesive is greater than that bonded by HMDS-treated-particle filled adhesive, irrespective of the particle contents and sizes. Fig. 9 shows the stress intensity factor for DCB specimens bonded by HMDS- and APDES-treated particles with various contents, where silica particle sizes are 6 and 30 μm. As shown in this figure, the difference of the stress intensity factor between two kinds of surface treatment does not vary with filler content, but increases with decreasing particle size.

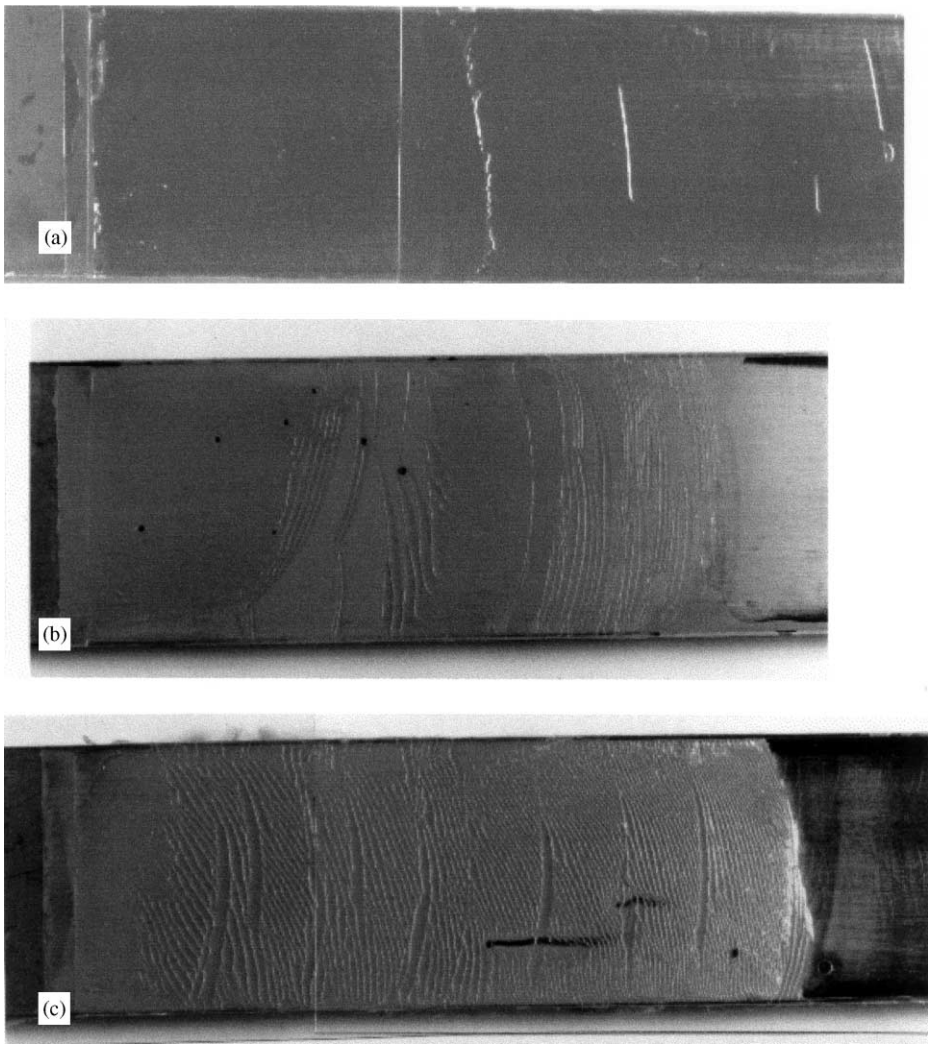

Fig. 7. Macroscopic view of fracture surfaces of DCB specimens bonded by silica-filled and unfilled adhesives: (a) unfilled adhesive, (b) HMDS-treated silica filled adhesive (mean size: 6μm, content: 25 wt%), (c) HMDS-treated silica filled adhesive (mean size: 30μm, content: 25 wt%).

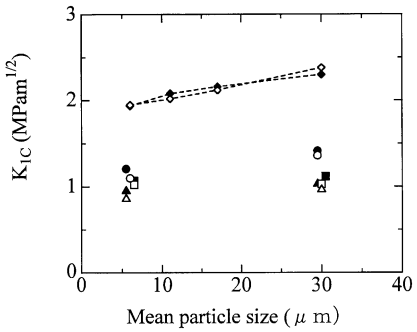

Fig. 8. Effect of surface treatment of silica particles on fracture toughness for the bulk and DCB specimens. Filled points are for APDES-treated silica particles and open points for HMDS-treated silica particles.

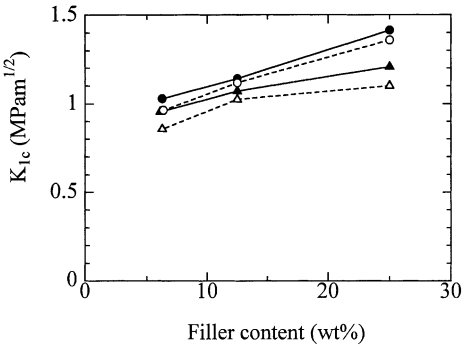

Fig. 9. Effect of silica content on the fracture toughness for a DCB specimen. Filled points are for APDES-treated silica particles and open points for HMDS-treated silica particles.

Generally, static tensile strength increases with increasing filler/matrix adhesion strength for many kinds of particle-filled composites. However, the fracture toughness of the filled composites does not necessarily increase with increasing filler/matrix adhesion strength. That is, a poorly bonded interface prompts debonding of silica particles, which leads to crack tip blunting due to local energy absorption. However, the pinning effect is weakened. A well bonded interface improves the efficiency of pinning, but

decreases local energy adsorption. The dependence of fracture toughness on particle/matrix adhesion is controlled by the balance between blunting and pinning. Hence, it would be expected from the experimental trends in Fig. 8 that the pinning effect may be more dominant than the crack tip blunting effect in the DCB specimens, while the pinning effect and blunting effect may be balanced in the bulk specimens. Furthermore as indicated in the previous section, the increase of silica content may diminish the efficiency of the pinning, but improve the crack tip blunting. In this experiment, the content of silica particles in bulk specimens was twice than that in DCB specimens. One reason the effect of surface treatment on fracture toughness differed between DCB and bulk specimens may be due to the difference in silica content.

Fig. 10 shows SEM images of fracture surfaces of DCB specimens bonded by HMDS- and APDES-treated silica particles. The holes which are traced from silica particles appear at the surface of HMDS-treated particles, whereas shallow holes appear at the surface of APDES-treated particles due to good particle/matrix adhesion which leads to crack propagation through the matrix above or below the poles of the particles. Such a trend has also been observed by Spanoudakis [6] and Kinloch [7] for bulk particle-filled resins. Hence, in the case of APDES-treated particles the crack propagation path is expected to be longer than that of HMDS-treated particles, where the fracture toughness increases with the crack propagation path. This may be one reason why the fracture toughness for the good particle/matrix adhesion system is higher than that for the system with poor adhesion for DCB specimens.

4. Conclusions

The fracture toughness of epoxy adhesive filled with spherical silica was measured using double cantilever

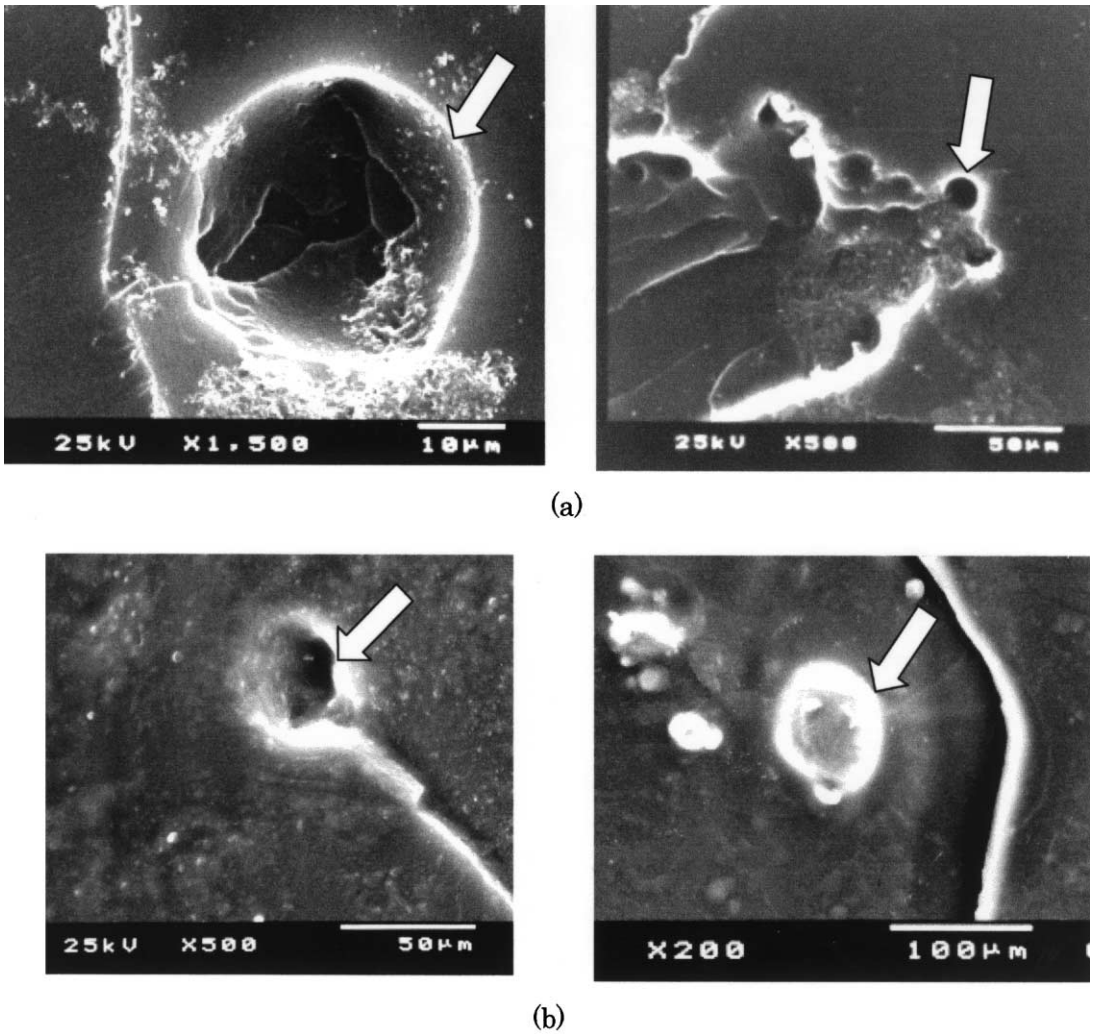

Fig. 10. Scanning electron micrographs of fracture surfaces of DCB specimens containing APDES- and HMDS-treated silica particles (mean size: 30 μm, content: 25 wt%); (a) HMDS-treated silica, (b) APDES-treated silica.

beam (DCB) specimens, where silica size, content and surface treatment of silica were varied. The main results are as follows:

1. Stick-slip type propagation behavior was observed for all DCB specimens.
2. Fracture toughness for both bulk and DCB specimens increased with particle size, where the effect of particle size on the fracture toughness strengthened with increasing content of particles. Fracture surfaces indicated that the density of irregular lines increased with particle size.
3. The ratios of K_{Ic} (silica filled)/K_{Ic} (unfilled) for both DCB and bulk specimens agree well with theoretical values obtained from the pinning theory at low volume content, whereas the scatter of the experimental data increases with volume content.
4. The fracture toughness for DCB specimens with good particle/matrix adhesion was slightly greater than for those with poor adhesion.

References

[1] Nielsen LE. Mechanical properties of polymers and composites. New York: Marcel Dekker Inc., 1975.
[2] Cantwell WJ, Roulin-Moloney AC. In: Roulin-Moloney AC, editor. Fractography and failure mechanisms of polymers and composites. Amsterdam: Elsevier, 1994. p. 233.
[3] Sahu S, Broutman LJ. Mechanical properties of particulate composites. Polym Eng Sci 1972;12:91–100.
[4] Radford KC. The mechanical properties of an epoxy resin with a second phase dispersion. J Mater Sci 1971;6:1286–91.
[5] Spanoudakis J, Young RJ. Crack propagation in a glass particle-filled epoxy resin, Part 1: effect of particle volume fraction and size. J Mater Sci 1984;19:473–86.
[6] Spanoudakis J, Young RJ. Crack propagation in a glass particle-filled epoxy resin, Part 2: effect of particle–matrix adhesion. J Mater Sci 1984;19:487–96.
[7] Kinloch AJ, Maxwell DL, Young RJ. The fracture of hybrid-particulate composites. J Mater Sci 1985;20:4169–84.
[8] Yaguchi A, Nishimura A, Kawai S. Fracture toughness measurement method and fracture properties of highly silica particle filled epoxy resins. J Math Soc Japan 1990;40:554–60 (in Japanese).
[9] Nishimura A, Yaguchi A. Effect of filler particle-size distribution on fracture toughness of silica particulate-filled epoxy resins. J Math Soc Japan 1991;41:1054–9 (in Japanese).
[10] Nakamura Y, Yamaguchi M, Kitayama A, Okubo M, Matsumoto T. Effect of particle size on fracture toughness of epoxy resin with angular-shaped silica. Polymer 1991;32:2221–9.
[11] Nakamura Y, Yamaguchi M, Okubo M, Matsumoto T. Effect of particle size on the fracture toughness of epoxy resin filled with spherical silica. Polymer 1992;33:3415–26.
[12] Evance AG. The strength of brittle materials containing second phase dispersions. Phil Mag 1972;26:1327–44.
[13] Green DG, Nicholson PS, Embury JD. Fracture of a brittle particulate composite, Part 2: theoretical aspects. J Mater Sci 1979;14:1657–61.
[14] Ward IM, Hadley DW. An introduction to the mechanical properties of solid polymers. New York: Wiley, 1993.
[15] Blackman B, Dear JP, Kinloch AJ, Osiyemi S. The calculation of adhesive fracture energies from double-cantilever bean test specimens. J Mater Sci Lett 1991;10:253–6.
[16] Nakamura Y, Okabe S, Imanaka M. Effect of interfacial adhesion on the flexural strength of spherical silica-filled epoxy resin. J Network Polym Jpn 1999;20:1–8 (in Japanese).
[17] Lange FF, Radford KC. Fracture energy of an epoxy composite system. J Mater Sci 1971;6:1197–203.
[18] Naito Y, Fujii T, Miyazaki Y. Surface topology and fractured surface of adhesives under static and fatigue loading. J Adhesion Soc Jpn 1994;30:299–306 (in Japanese).